

The energy gap of intermediate-valent SmB_6 studied by point-contact spectroscopy

K. Flachbart^{a,*}, K. Gloos^{b,c}, E. Konovalova^d, Y. Paderno^d, M. Reiffers^a, P. Samuely^a, P. Švec^e

^a*Institute of Experimental Physics, Slovak Academy of Sciences, SK-04353 Košice, Slovakia*

^b*Institut für Festkörperphysik, Technische Universität Darmstadt, D-64289 Darmstadt, Germany*

^c*Department of Physics, University of Jyväskylä, FIN-40351 Jyväskylä, Finland*

^d*Institute for Problems of Materials Science, UA-252680 Kiev, Ukraine*

^e*Institute of Physics, Slovak Academy of Sciences, SK-84228 Bratislava, Slovakia*

(October 24, 2018)

We have investigated the intermediate valence narrow-gap semiconductor SmB_6 at low temperatures using both conventional spear-anvil type point contacts as well as mechanically controllable break junctions. The zero-bias conductance varied between less than $0.01 \mu\text{S}$ and up to 1 mS . The position of the spectral anomalies, which are related to the different activation energies and band gaps of SmB_6 , did not depend on the the contact size. Two different regimes of charge transport could be distinguished: Contacts with large zero - bias conductance are in the diffusive Maxwell regime. They had spectra with only small non-linearities. Contacts with small zero - bias conductance are in the tunnelling regime. They had larger anomalies, but still indicating a finite 45% residual quasiparticle density of states at the Fermi level at low temperatures of $T = 0.1 \text{ K}$. The density of states derived from the tunnelling spectra can be decomposed into two energy-dependent parts with $E_g = 21 \text{ meV}$ and $E_d = 4.5 \text{ meV}$ wide gaps, respectively.

PACS numbers: 71.28.+d, 71.30.+h, 75.30.Mb

I. INTRODUCTION

Samarium hexaboride SmB_6 is a homogeneous intermediate - valence compound in which the electronic structure at low temperatures shows a narrow energy gap as well as spin gap, both originating from the hybridization between the narrow states formed by electrons of samarium $4f$ - shell and the wide conduction band formed by both boron p - states and $\text{Sm } 6s$ - states [1]. A review of this and similar materials can be found in Refs. [1–4].

Recent experiments on SmB_6 [5–13] have shown that in the low-energy excitation spectrum of this material several energy scales exist, and also several regimes of low-temperature electron kinetics. At least three different activation energies determine the behaviour of the conduction electrons. In the temperature range $70 \text{ K} > T > 15 \text{ K}$ the properties of SmB_6 are governed by the hybridization gap $E_g \approx 10 - 20 \text{ meV}$. Between 15 K and 5 K , a narrow in - gap band separated from the bottom of the conduction band by a direct activation energy of $E_d \approx 3 - 5 \text{ meV}$ has been observed. The properties of this narrow band seem to be influenced by the content of impurities and imperfections of the specific sample. Below about 5 K the electrical conductivity saturates, indicating a small conductivity channel within the E_d in - gap states, where the Fermi level is pinned.

Various models have been proposed to explain the formation of the E_d - band and the origin of the residual conductivity [3,14–21], but so far no final conclusion could be obtained. While Ref. [12] favours hopping processes of electrons, Refs. [22,23] prefer a coherent metal-like state at low temperatures. In either case electrons are strongly localized ($\sim 0.6 \text{ nm}$ localisation radius) at random impu-

rities with a small concentration of $N \approx 10^{23} \text{ m}^{-3}$ at low temperatures [22].

To search for anomalies in the quasi-particle density of states a number of experiments on small junctions with SmB_6 has been performed. Frankowski and Wachter [24] brought a sharply etched molybdenum tip into direct contact with the surface of a cleaved SmB_6 single crystal. The spectra of these low-resistance contacts showed a 4.6 meV wide anomaly (full width at half maximum) which was attributed to a gap in the density of states. The overall size of this anomaly was only about 10% of the mean contact resistance. Güntherodt *et al.* [25] investigated Schottky-type tunnel contacts between SmB_6 and GaAs . They found a huge but only 2.7 meV wide zero-bias anomaly. Such small gaps were obtained only when the SmB_6 surface was sputter cleaned *in situ*. Without such a treatment the anomalies broadened to around 10 meV . Planar tunnel junctions with lead counter electrodes were investigated by Batlogg *et al.* [26] and by Amsler *et al.* [27]. The latter experiments showed 14 meV wide spectral anomalies, roughly coinciding with the E_g band gap, and a $\sim 70\%$ residual quasiparticle density of states at the Fermi level. No consistent picture could evolve from all these experiments, because the width as well as the size of the main zero-bias anomaly varied a lot. To obtain more and, hopefully, reliable information on the different energy scales involved we investigated direct junctions between two bulk pieces of SmB_6 as function of contact size.

II. EXPERIMENTAL

Our SmB₆ samples were cut from one batch which was grown by the zone-floating method as described in Ref. [28]. About 800 ppm magnetic impurities, mostly magnetic lanthanide elements close to Sm in the periodic table, were found by magnetic susceptibility measurements [10]. A similar amount of non-magnetic impurities, mainly lanthanum, was detected by induction-coupled plasma spectroscopy. sufficient size.

Two different type of point contacts were prepared. First, two mechanically polished pieces of SmB₆ were brought into contact in a spear-anvil type setup and measured at 4.2 K in liquid helium. Second, bulk pieces of SmB₆ were broken at a predefined notch in the ultrahigh vacuum region of a cold ³He-⁴He dilution refrigerator and measured mainly at 0.1 K. Reference [29] describes our break-junction apparatus in detail. With mechanically-controllable break junctions we avoid the oxidation of the interfaces. It also offers excellent mechanical stability of the contacts so that also very small junctions can be investigated. In both cases the $dI/dU(U)$ spectra were recorded in the standard four-terminal mode with current biasing.

III. ELECTRICAL CONDUCTIVITY AND ACTIVATION ENERGIES

Figure 1 shows the temperature dependence of the bulk conductivity $\sigma(T)$ of the single crystalline SmB₆ sample. $\sigma(T)$ decreases in a rather complicated way with decreasing T , saturating at the lowest temperatures. Describing the conductivity by thermally activated mechanism, $\sigma(T) \propto \exp(-W/k_B T)$, an activation energy

$$W = -d(\ln \sigma(T))/d(1/k_B T) \quad (1)$$

can be defined (Fig. 2). It shows a peak of about 5.6 meV in the temperature range between 70 K and 15 K. This value can be attributed to $E_g^*/2$ when the Fermi level sits just in the center of the hybridization band gap of width $E_g^* \approx 11.2$ meV. Between 15 K and 5 K the second pronounced peak appears. Its value of $E_d^* \approx 3.7$ meV corresponds to the formation of the narrow in-gap band within the hybridization gap located E_d^* below the conduction band edge. These two activation energies do not clearly level off. Therefore the index '*' is used to distinguish the activation-derived values from the true energy gaps still to be determined.

With further decreasing temperature, the activation energy W falls to very low values. The anomaly at about 1 – 2 K with $E_a \approx 0.2$ meV originates probably from an additional narrow band formed inside the energy gap (close to the E_d -band) due to the relatively large content of impurities of the sample. Below about 1 K, however,

the activation energy is lower than the available thermal energy $k_B T$, indicating a metallic-like conduction mechanism at the lowest temperatures. This would agree with recent ac -conductivity [22] and specific heat measurements of SmB₆ [23], which are interpreted as showing a transition into a coherent heavy-fermion like state below about 5 K.

IV. POINT-CONTACT SPECTROSCOPY

We have investigated more than 100 SmB₆ - SmB₆ point contacts with zero-bias conductance ranging from about 0.01 μS to about 1 mS, most of them using the spear-anvil technique. These spear-anvil type junctions had a high zero-bias conductance and usually symmetric $dI/dU(U)$ spectra, similar to those obtained earlier on SmB₆ - Mo point contacts [24]. But few of those junctions were asymmetric like that in Figure 3. We found anomalies, typically small kinks in the dI/dU spectra indicating a change of slope, at $U \approx 4$ mV and $U \approx 12$ mV, respectively.

Figures 4, 5, and 6 show typical dI/dU spectra of SmB₆ break junctions at $T = 0.1$ K. Like the spear-anvil type contacts they had anomalies in dI/dU and in d^2I/dU^2 at about 4 mV and 12 meV. Very often additional anomalies were observed close to 0.2 mV, 1.8 mV, and 22 meV. Several junctions also had anomalies at about 80 mV.

Spectra with high zero-bias conductance $G_0 = dI/dU(T = 0.1 \text{ K}, U = 0)$ shown in Fig. 4 were symmetric with respect to the applied voltage. Figs. 5 and 6 show that when the zero-bias conductance G_0 falls below about 30 μS , the differential conductance becomes more and more asymmetric. This tendency towards asymmetry could result from an inhomogeneous distribution of impurities and imperfections in the sample which can lead to different local carrier concentration, and which become the more pronounced the smaller the contact interface is. The different possible crystallographic orientations of the SmB₆ electrodes forming the contact could also contribute to the asymmetry.

The spectra of junctions with low conductance (Fig. 6) appear to be broader than those with higher zero-bias conductance (Fig. 5). However, according to Fig. 7 the position of the anomalies is not affected by any variation of G_0 . This points then to different weighing factors of the anomalies at small and at large zero-bias conductance, respectively, possibly reflecting the two different regimes of charge transport discussed below. In Fig. 7 we have labeled the positions according to the activation energies E_a , E_d^* , and E_g^* . Anomalies around 1.8 mV as well as around 22 meV could be related with $E_g^*/2 - E_d^*$ and $2E_g^*$, respectively. And one could speculate whether the 80 mV anomalies (not shown in the figure) correspond to the excitation of electrons into higher energy levels of the

Sm - ions, considered for example to interpret magnetic properties of SmB₆ [1,30].

The properties of the junctions depend only weakly on temperature (Fig. 8) and on magnetic field (Fig. 9). In both cases, the shape of the spectra does not change much, only the conductance increases slightly when either the temperature is raised from 0.1 K to 1 K or the magnetic field from 0 Tesla to 8 Tesla (the field was always perpendicular to the direction of current flow). Thus also the magneto resistance is small and negative like in the bulk sample. Junctions with large zero-bias conductance $G_0 \approx 1 \text{ mS}$ had typically $G_0(B = 0)/G_0(B) - 1 \approx -1.3 \times 10^{-3} B^2$, where B is the applied field in Tesla (Fig. 10).

V. REGIMES OF CHARGE TRANSPORT

To evaluate the observed $dI/dU(U)$ dependencies not only qualitatively, one should know the regime of charge transport across the contacts. This is absolutely necessary if one wants to attribute a spectral anomaly at a bias voltage U to an anomaly in the density of states or to some scattering mechanism at an energy eU . We face here a quite general – but very often ignored – problem of direct contacts (that means contacts without well-defined tunneling barrier) between conductors with a short electronic mean free path. Naidyuk and Yanson [31] have recently reviewed and discussed this topic.

As one typical example to illustrate the situation we refer to point-contact experiments with the Kondo semiconductor CeNiSn. It is usually believed that direct junctions with this short mean free path compound are in the tunnelling regime, implying that the spectra measure the density of states [32,33]. However, it was demonstrated recently that those point contacts are more likely metallic [34]. And this, in turn, makes it impossible to extract the density of states.

We emphasize that the shape of the spectra itself does not tell anything about the regime of charge transport, whether it is tunnelling or diffusive transport, for example, unless one works with a well-known substance for which the spectra can be predicted reliably. Experiments with a superconducting lead counter electrode like that in Ref. [27] allow the quality of a tunnel junction to be verified. For such an experiment quantum tunneling can be confirmed or disproved. Obviously, this does not work for SmB₆ in contact with an other piece of SmB₆, since the exact properties of this compound have yet to be determined. Thus for our experiments the situation seems hopeless. But there exists what we believe are strong arguments to identify the relevant transport mechanisms. We use a procedure that has been developed for contacts with heavy-fermion compounds [35,36] as well as for junctions with doped germanium [37,38], both materials with

a typically short electronic mean free path (or hopping length in the latter case).

VI. LARGE JUNCTIONS – MAXWELL REGIME

SmB₆ has – due to hybridization effects – an extremely short electronic mean free path at low temperatures, which amounts to not more than several lattice constants. Therefore it is difficult to evaluate our experiments in terms of the classical metallic point contact spectroscopy. When the diameter d , the characteristic dimension of the point-contact, is large, it can certainly be estimated using Maxwell’s formula $G \approx \sigma d$, where $G = dI/dU$ is the point-contact conductance at zero bias (a circular shape of the contact is a useful simplifying assumption). Two approaches are possible: One could set G of Maxwell’s formula equal to the measured $dI/dU(U = 0)$ and use the measured σ at the same temperature. Thus, with $\sigma(T = 0.1 \text{ K}) \approx 0.05 \mu\text{S/cm}$ from Fig. 1, a $G_0 = 1 \mu\text{S}$ junction has a $d \approx 200 \text{ nm}$ diameter. However, it is better – and this has been clearly demonstrated for junctions with the heavy-fermion superconductors [35,36] – to use the change of conductance δG and conductivity $\delta\sigma$, respectively, when the temperature is increased. Thus the contact diameter in the Maxwell regime actually becomes

$$d \approx \delta\sigma/\delta G. \quad (2)$$

We have noted that the conductance increases by roughly 5 % when the temperature is increased from 0.1 to 1 K. At the same time, the bulk conductivity of our sample increases by a factor of 4 to about 0.2 S/cm. If we attribute this increase of conductance to the increase of bulk conductivity in Fig. 1 then, according to Eq. 2, the diameter amounts to about 3 nm only. (Applying this method on SmB₆ is by far less reliable than for junctions with the heavy-fermion compounds. The above value should be regarded as an estimate for the order of magnitude of d .) Such a small contact is still formed by ~ 100 atoms which contribute to its mechanical stability. In fact, we have found a lack of stability, indicating the transition to ‘one atom’ junctions, only when the conductance is further reduced by a factor of at least 100. This qualitative agreement supports our estimate of the contact size. Nevertheless, Maxwell’s formula is valid only for large junctions, and we have yet to determine its lower bound.

The large temperature-independent background needs to be explained: It is not due to impurities of the bulk sample. More likely the contact distorts the crystal lattice locally, and these additional defects enhance the local conductivity. A similar phenomenon – but of opposite direction – has been observed at junctions with heavy-fermion materials [35,36]. Lattice defects there enhance the local resistivity and, consequently, the contact resistance. Using the absolute value of the contact resistance

itself instead of its temperature-dependent part would then considerably underestimate the contact diameter, contrary to the SmB₆ junctions.

Joule heating of our SmB₆ - SmB₆ contacts could be expected at high bias voltages. A simple heating model [39] predicts the effective temperature of the contact

$$T_{eff} = \sqrt{T_b^2 + U^2/4L} \quad (3)$$

at a bath temperature T_b . Here the Lorenz number $L = \kappa/\sigma T$, and κ denotes the thermal conductivity of the material in the contact region. In the Drude - Sommerfeld theory of metals L equals $L_0 = 2.45 \times 10^{-8} \text{ V}^2/\text{K}^2$, implying a significant overheating of the contact. However, SmB₆ has a very low electrical conductivity below about 5 K (Fig. 1) but a rather high thermal conductivity [40] due to heat transport by phonons. This yields a more than five orders of magnitude higher L and provides a very effective cooling of the contact. Electrons crossing such a large junction take part in many scattering events, but basically they keep their original kinetic energy as they diffuse through the contact region. At a bath temperature of $T_b = 0.1 \text{ K}$ a voltage of $U = 30 \text{ mV}$ would heat up the contact to not more than $T_{eff} \approx 0.4 \text{ K}$. Therefore the applied voltage U is too small to account for any of the observed anomalies of the dI/dU spectra in terms of overheating, and the observed anomalies should mark the correct energies at which certain energy bands can be occupied or scattering mechanisms start to work.

The small magnetoresistance, less than 10% at $B = 8 \text{ Tesla}$ for the junction in Fig. 9, also indicates no overheating. Otherwise a much larger effect had to be expected from the strong magnetoresistivity of the bulk sample above 1 K.

VII. SMALL JUNCTIONS – TUNNELLING

On further reducing the lateral size or diameter of the junctions one should expect a transition to ballistic transport if SmB₆ was an ordinary metal. Obviously, this is not the case. Because of the low carrier concentration of $N \approx 10^{23} \text{ m}^{-3}$ [22], the junctions will instead undergo a transition to tunnelling. Again there are two different approaches to estimate the contact diameter at which this transition will take place, depending on whether conduction is due to electrons in a coherent metal-like state or due to hopping.

First, if the electron system at low temperatures is described by a coherent state, the Fermi wave number amounts to about $k_F = (3\pi N)^{1/3} = 10^8 \text{ m}^{-1}$. In the contact region, discrete energy levels can exist which carry electrical current as long as the contact diameter d is larger than $4/k_F \approx 40 \text{ nm}$. If the diameter is smaller, electrons have to cross the junction as evanescent waves,

that means they tunnel. Such a situation has been observed at direct junctions with antimon, also a compound with a low carrier density [41].

Second, if electron transport is due to thermally activated hopping between localized impurity states as proposed in Ref. [12], for example, then junctions with SmB₆ should be compared with those of a real semiconductor like germanium. Junctions with doped Ge seem to be in a tunnelling state although there is a direct contact with the bulk material without dielectric barrier [37,38]. Transport across such contacts can be called 'tunnelling' because the hopping length is so large that the charge carriers cross the junction interface by one single hop process. These hop processes across the junction are the same as that in the bulk material. We believe that our SmB₆ junctions with small zero-bias conductance can be in such a tunneling-like state. A reasonable estimate for the impurity density is the carrier density, and the average distance between the impurities equals the hopping length. The transition to tunneling has then to be expected when the contacts become smaller than $N^{-1/3} \approx 22 \text{ nm}$.

For both approaches, using Eq. 2 to estimate the contact diameter, the transition towards tunnelling should take place when the zero-bias conductance gets smaller than about $10 \mu\text{S}$. And this is just what we are observing: a transition in the size of the zero-bias anomalies when G_0 is reduced. We fit a parabola to the spectra at high voltages as indicated in Fig. 4 to define as reference the conductance at zero bias G_H if there was no gap in the density of states. (According to Ref. [27] one would have to increase the temperature of a specific junction to above 40 K to get an experimental value for G_H . This was not possible with our apparatus). The relative size of the zero-bias anomaly at low temperatures is then G_0/G_H . For contacts between SmB₆ and a normal metal with constant density of states around the Fermi level, like that in Ref. [27], the differential conductance $dI/dU(U)$ is proportional to the energy dependence of the local electronic density of states multiplied by the transmission probability of the contact [42]. Thus $g_0/g_H \approx G_0/G_H$ when g_0 , the low-temperature density of states at the Fermi level, is normalized to the density of states without gap g_H . Since for SmB₆ - SmB₆ homocontacts the same quasiparticle density of states on both sides of the contact contribute to the tunnel conductance, g_0 has to be described by

$$g_0/g_H \approx \sqrt{G_0/G_H} \quad (4)$$

Fig. 11 shows that large junctions (large G_0) also have large $\sqrt{G_0/G_H}$ because of their large background signal. This is inconsistent with the quasiparticle density of states of around 70% measured using planar tunnel junctions at $T = 10 \text{ K}$ [27]. Moreover there seems to be a systematic decrease of the relative size of the anomaly as

$G_0 \rightarrow 1 \text{ mS}$, possibly indicating a transition from diffusive to thermal transport when progressively more scattering processes are required for an electron to pass the contact region. Its initial kinetic energy is then not conserved any more. The signal size of smaller junctions, however, agrees much better with the expected density of states if we take into account our much lower temperatures of $T = 0.1 \text{ K}$, letting us attribute the zero-bias conductance to the finite density of quasi-particles in the gap at the Fermi level. Thus bulk transport turns to tunneling below about $G_0 \approx 2 \mu\text{S}$, in excellent agreement with our above estimate.

VIII. THE ENERGY GAPS AND THE QUASIPARTICLE DENSITY OF STATES

Most of the anomalies, for the break junctions as well as for the spear-anvil type contacts, were found at positions that coincide well with the characteristic activation energies of SmB_6 (Fig. 7). The important point here is that, whatever the interpretation of these energies: the positions do not depend on the zero-bias conductance, that means on the lateral contact size. It implies that there is no additional voltage drop in the contact area, which could pose a problem at very large junctions with $G_0 \geq 1 \text{ mS}$. Thus Fig. 7 demonstrates that at least up to $G_0 \approx 1 \text{ mS}$ we can still derive the kinetic energy of the electrons from the applied bias voltage because of the suppressed local heating.

Anomalies at E_g^* as well as at E_d^* could be observed at all junctions. These dominant anomalies could indicate when the top of the valence band and the narrow impurity band of one electrode, respectively, face the bottom of the conduction band of the other electrode. At some junctions we could also resolve a small anomaly which corresponds to the lowest activation energy E_a of our sample. It may represent an additional impurity band close to the E_d band.

Not all junctions showed anomalies at around 0.2 meV , 2 meV , and 22 meV . An obvious reason for the sometime missing low-energy anomalies could be the degradation of the interface region due to the contact, increasing the local conductivity and thereby suppressing the low-energy processes. Two of the anomalies, the one at 1.8 meV and the other at 22 meV , have no counterpart as an activation energy from Fig. 2. And it is unclear whether they just accidentally coincide with $E_g^*/2 - E_d^*$ and $2E_g^*$, respectively. To speculate whether the anomaly at twice E_g^* results from a double junction, that is a contact with two junctions in series, can be safely discarded because there are no corresponding anomalies at lower energies at $2E_d^*$ or at $2E_a$. The two above anomalies could be artefacts, created by the stress in the contact region, and which is not present in the bulk sample. But there is no reason why in such a case the position of the other

anomalies should not be affected in a similar way. This open question leads us to reconsider our way of attributing certain energies derived from the activation energy to the observed anomalies.

The necessary additional information can be obtained from the tunnelling spectra. As discussed above, a residual quasiparticle density of states at the Fermi level of about 45%, derived from the size of the zero-bias anomalies of small junctions with $G_0 \leq 1 \mu\text{S}$ and shown in Fig. 11, is considerably smaller than the data obtained by conventional tunnel junctions [27]. However, this difference is not unreasonable because the latter experiments, compared to ours, were carried out at much higher temperatures when the E_d anomaly has not fully developed. The rather large scattering of our data points in Fig. 11 probably results, in a minor part, from our method of extrapolating G_H , the zero-bias conductance without gap. The major part is due to the fact that the break junctions are a local probe. Each junction has slightly different local properties, for example due to stress induced by the contact. At planar tunnel junctions, on the other hand, the density of states is sampled and averaged over a much wider contact area. Of course, uniform stress and a preferred direction could affect the spectra of those planar junctions as well.

To estimate the average density of states at our SmB_6 tunnel junctions, that means junctions with $G_0 \leq 1 \mu\text{S}$, we normalized their spectra with respect to the voltage-dependent background as described in Fig. 4, averaged the normalized spectra, and then fitted the average spectrum by various functional dependencies of the density of states, assuming a constant transmission probability. A good fit was obtained by assuming a constant background of 45% and two different energy-dependent parts $g_{1,2}(E)$ of the density of states as shown in Fig. 12.

The one part, $g_1(E)$, has a rather wide gap of about 21 meV (full width at half maximum), while the other part, $g_2(E)$, has a much narrower gap of about 4.5 meV . These two gaps may be attributed to the hybridization gap and the E_d anomaly, respectively. But in this case the width of the larger anomaly differs a lot, almost a factor of two, from the activation energy data. On the other hand, if the gap in $g_2(E)$ was suppressed, leaving only the gap in $g_1(E)$, the anomaly of the density of states found in Ref. [27] for planar SmB_6 - Pb tunnel junctions at 10 K would be reproduced quite well (the anomaly described by Ref. [27] had a somewhat smaller width of about 14 meV , possibly because it was also asymmetric). This supports our interpretation of tunnelling due to the lateral confinement at our junctions. It seems as if the gap in $g_2(E)$ develops only at low temperatures $T \ll 10 \text{ K}$. And this has to be expected in view of the bulk conductivity and the activation energy.

The second derivative d^2I/dU^2 of the average spectrum as well as of the fit in Fig. 13 clearly show anomalies at around 1.6 mV , 5.5 mV , 11 mV , and 21 mV , respec-

tively. Thus except for $E_a = 0.2\text{ eV}$ all anomalies found in the spectra as displayed in Fig. 7 can also be recovered from the fit curve. We believe that the activation-derived gaps differ from the real gap values $E_g = 21\text{ meV}$ and $E_d = 4.5\text{ meV}$ because even at low temperatures the density of states remains finite inside the gaps. Therefore electrons can be thermally excited into states with energy $E \leq E_d$ or $E \leq E_g/2$, respectively, smearing out the otherwise discrete activation-energy levels.

IX. CONCLUSION

The differential conductance of SmB_6 - SmB_6 junctions has been investigated at low temperatures as function of contact size. A very wide range of data on the conductance scale down to very small junctions was made possible because of the excellent mechanical stability of the break junctions when compared to the spear-anvil type contacts. Two different regimes of charge transport were distinguished. Large junctions are in the diffusive Maxwell regime, in which the conductance is dominated by the bulk conductivity. Local heating is negligible because of the large phonon heat conductivity. Therefore, the applied bias voltage can still be attributed to the kinetic energy of the charge carriers, enabling spectroscopy. Small junctions are in the tunnelling regime, although there is no dielectric barrier. Depending on the model used, electrons tunnel through the contact either by a single hopping event like in the bulk material or as evanescent waves because of a large Fermi wavenumber. Both models predict the transition to tunnelling when the zero-bias conductance becomes smaller than about $10\text{ }\mu\text{S}$, in good agreement with our experiments. The spectra of these tunnel junctions indicate a finite 45% residual density of states at the Fermi level. In the two different regimes of transport, at large as well as at small junctions, anomalies can be resolved at the same energies. However, only the spectra in the tunnelling regime reveal the correct gaps in the density of states of $E_g = 21\text{ meV}$ and $E_d = 4.5\text{ meV}$ that are responsible for the observed anomalies. The absolute values of these two energies fit well those derived from other experiments.

X. ACKNOWLEDGMENTS

This work was supported by the Slovak Scientific Grant Agency VEGA, contract 1148 - 01 and 7022 - 20, and by the SFB 252 Darmstadt / Frankfurt / Mainz. US Steel Košice sponsored part of the liquid nitrogen.

- [1] P. Wachter in: *Handbook on the Physics and Chemistry of Rare Earths*, edited by K. A. Gschneidner, Jr. and L. Eyring, North-Holland, Amsterdam, 1994, Vol. 19, p. 177.
- [2] G. Aeppli and Z. Fisk, *Comments Cond. Mat. Phys.* **16**, 155 (1992).
- [3] T. Kasuya, *Europhys. Lett.* **26**, 277 (1994); T. Kasuya, *Europhys. Lett.* **26**, 283 (1994).
- [4] P. S. Riseborough, *Adv. Phys.* **49**, 257 (2000).
- [5] I. Bat'ko, P. Farkašovský, K. Flachbart, E. S. Kononova, and Yu. B. Paderno, *Solid State Commun.* **88**, 405 (1993).
- [6] T. Nanba, H. Ohta, M. Motokawa, S. Kimura, S. Kunii, and T. Kasuya, *Physica B* **186-188**, 440 (1993).
- [7] J. C. Cooley, M. C. Aronson, Z. Fisk, and P. C. Canfield, *Phys. Rev. Lett.* **74**, 1629 (1995).
- [8] J. C. Cooley, M. C. Aronson, A. Lacerda, Z. Fisk, P. C. Canfield, and R. P. Guertin, *Phys. Rev.* **52**, 7322 (1995).
- [9] P. Nyhus, S. L. Cooper, Z. Fisk, and J. Sarrao, *Phys. Rev.* **55**, 12488 (1997).
- [10] J. Roman, V. Pavlík, K. Flachbart, T. Herrmannsdörfer, S. Rehmann, E. S. Kononova, and Yu. B. Paderno, *Physica B* **230-232**, 715 (1997).
- [11] N. E. Sluchanko, A. A. Volkov, V. V. Glushkov, B. P. Gorshunov, S. V. Demishev, M. V. Kordin, A. A. Pronin, N. A. Samarin, Y. Bruynseraede, V. V. Moshchalkov, and S. Kunii, *J. Exp. Theor. Phys.* **88**, 533 (1999).
- [12] B. Gorshunov, N. Sluchanko, A. Volkov, M. Dressel, G. Knebel, A. Loidl, and S. Kunii, *Phys. Rev. B* **59**, 1808 (1999).
- [13] M. Dressel, B. P. Gorshunov, N. E. Sluchanko, A. A. Volkov, B. Hendersen, G. Grüner, G. Knebel, A. Loidl, and S. Kunii, *phys. stat. sol. B* **215**, 161 (1999).
- [14] J. W. Allen, B. Batlog, and P. Wachter, *Phys. Rev. B* **20**, 4807 (1979).
- [15] N. F. Mott in: *Valence Instabilities*, edited by P. Wachter and H. Boppert, North-Holland, Amsterdam 1982, p. 397 and p. 403.
- [16] T. Kasuya, K. Takegahara, T. Fujita, T. Tanaka, and E. Banai, *J. Phys. (Paris) Colloq.* **40**, C5-308 (1979).
- [17] K. A. Kikoin and A. S. Mishchenko, *J. Phys.: Condens. Matter* **7**, 307 (1995).
- [18] S. Curnoe and K. Kikoin, *Physica B* **284-288**, 1357 (2000).
- [19] K. Hanzawa, *J. Phys. Soc. Jpn.* **67**, 3151 (1998).
- [20] A. Kebede, M. C. Aronson, C. M. Buford, P. C. Canfield, J. H. Cho, B. R. Coles, J. C. Cooley, J. Y. Coulter, Z. Fisk, J. D. Goettee, W. L. Hults, A. Lacerda, T. D. McLendon, P. Tiwari, and J. L. Smith, *Physica B* **223&224**, 256 (1996).
- [21] M. Park and J. Hong, *J. Korean Phys. Soc.* **33**, 480 (1998).
- [22] N. E. Sluchanko, V. V. Glushkov, B. P. Gorshunov, S. V. Demishev, M. V. Kordin, A. A. Pronin, A. A. Volkov, A. K. Savchenko, G. Grüner, Y. Bruynseraede, V. V. Moshchalkov, and S. Kunii, *Phys. Rev. B* **61**, 9906 (2000).
- [23] S. Gabáni, K. Flachbart, E. Kononova, M. Orendáč, Y. Paderno, V. Pavlík and J. Šebek, *Solid State Com-*

- mun. **117**, 641 (2001).
- [24] I. Frankowski and P. Wachter in: *Valence Instabilities*, Editors P. Wachter and H. Boppert, North - Holland Publ. Co., Amsterdam 1982, p. 309; Solid State Commun. **41**, 577 (1982).
 - [25] G. Güntherodt, W. A. Thompson, F. Holzberg, and Z. Fisk, Phys. Rev. Lett. **49**, 1030 (1982).
 - [26] B. Batlogg, P. H. Schmidt, and J. M. Rowell in: *Valence Fluctuations in Solids*, Edited by W. Hanke and M. B. Maple, North - Holland, Amsterdam 1981, p. 267.
 - [27] B. Amsler, Z. Fisk, J. L. Sarrao, S. von Molnar, M. W. Meisel, and F. Sharifi, Phys. Rev. **B 57**, 8747 (1998).
 - [28] E. S. Kononova, Yu. B. Paderno, S. I. Liukshina, and E. V. Yuhimenko, Inorgan. Mater. **26**, 1218 (1990) (in Russian).
 - [29] K. Gloos and F. Anders, J. Low Temp. Phys. **116**, 21 (1999).
 - [30] J. C. Nickerson, R. M. White, K. N. Lee, R. Bachmann, T. H. Geballe, and G. W. Hull, Jr., Phys. Rev. **B 3**, 2030 (1971).
 - [31] Yu. G. Naidyuk and I. K. Yanson, J. Phys.: Cond. Matter **10**, 8905 (1998).
 - [32] T. Ekino, T. Takabatake, H. Tanaka, and H. Fujii, Phys. Rev. Lett. **75**, 4262 (1995).
 - [33] D. N. Davydov, S. Kambe, A. G. M. Jansen, P. Wyder, N. Wilson, G. Lapertot, and J. Flouquet, Phys. Rev. **B 55**, 7299 (1997).
 - [34] Yu. Naidyuk, K. Gloos, and T. Takabatake, Low Temp. Phys. **26**, 502 (2000) [Fiz. Nizk. Temp. **26**, 687 (2000)].
 - [35] K. Gloos, F. B. Anders, B. Buschinger, C. Geibel, K. Heuser, F. Jährling, J. S. Kim, R. Klemens, R. Müller-Reisener, C. Schank, and G. R. Stewart, J. Low Temp. Phys. **105**, 37 (1996).
 - [36] K. Gloos, F. B. Anders, W. Assmus, B. Buschinger, C. Geibel, J. S. Kim, A. A. Menovsky, R. Müller-Reisener, S. Nuettgens, C. Schank, G. R. Stewart, and Yu. G. Naidyuk, J. Low Temp. Phys. **110**, 873 (1998).
 - [37] B. Sandow, K. Gloos, R. Rentzsch, and A. N. Ionov, Physica **B 284**, 1852 (2000).
 - [38] B. Sandow, K. Gloos, R. Rentzsch, A. N. Ionov, and W. Schirmacher, Phys. Rev. Lett. **86**, 1845 (2001).
 - [39] I. O. Kulik, Sov. J. Low Temp. Phys. **18**, 302 (1992) [Fiz. Nizk. Temp. **18**, 450 (1992)].
 - [40] K. Flachbart, M. Reiffers, Š. Jánoš, Yu. B. Paderno, V. I. Lazorenko, and E. S. Kononova, J. Less-Comm. Met. **88**, L11 (1982).
 - [41] J. M. Kras and J. M. van Ruitenbeek, Phys. Rev. **B 50**, 17659 (1994).
 - [42] F. A. Padovani in: *Semiconductors and Semimetals*, Edited by R. Willardson and A. Beer, Academic, New York 1971, p. 75.

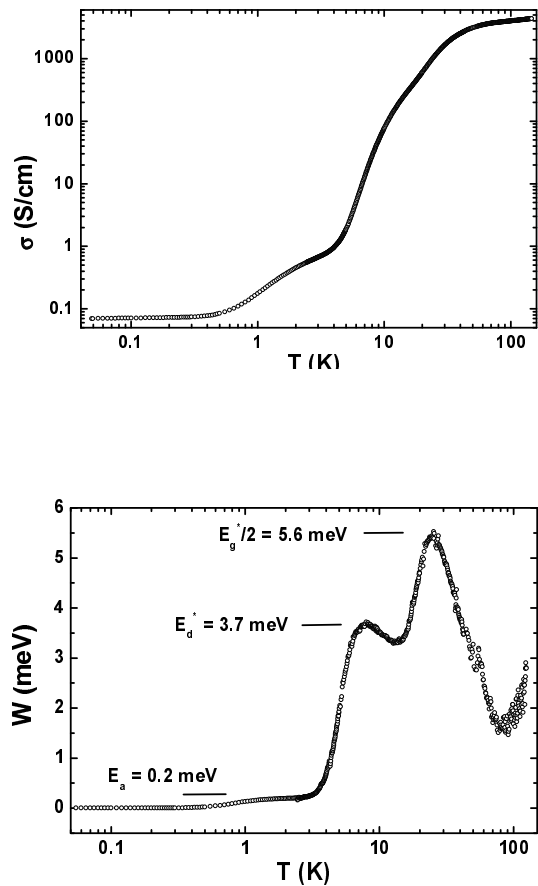


FIG. 2. Temperature dependence of the activation energy W

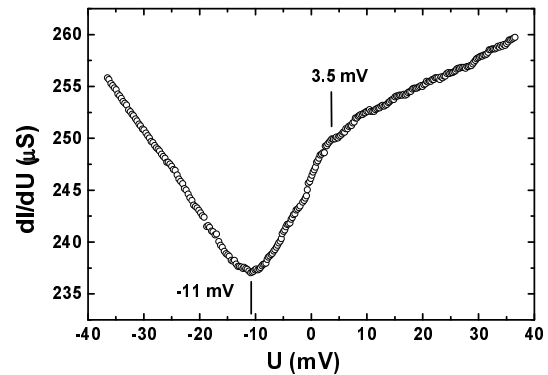


FIG. 3. Symmetric (top) and asymmetric (bottom) $dI/dU(U)$ spectra of spear-anvil type contacts with high zero-bias conductance. $T = 4.2$ K.

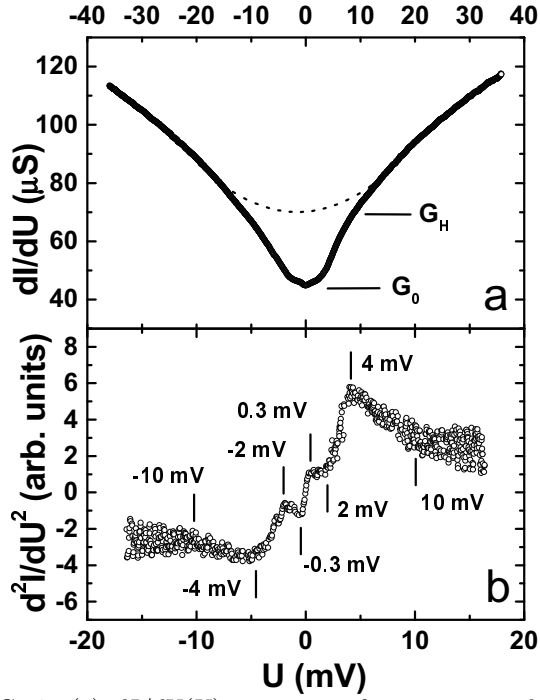


FIG. 4. (a) $dI/dU(U)$ spectrum of a contact with high zero-bias conductance $G_0 = dI/dU(U = 0)$ at $T = 0.1$ K. The dotted line describes tentatively the expected spectrum at high temperatures with zero-bias conductance G_H . (b) Seco

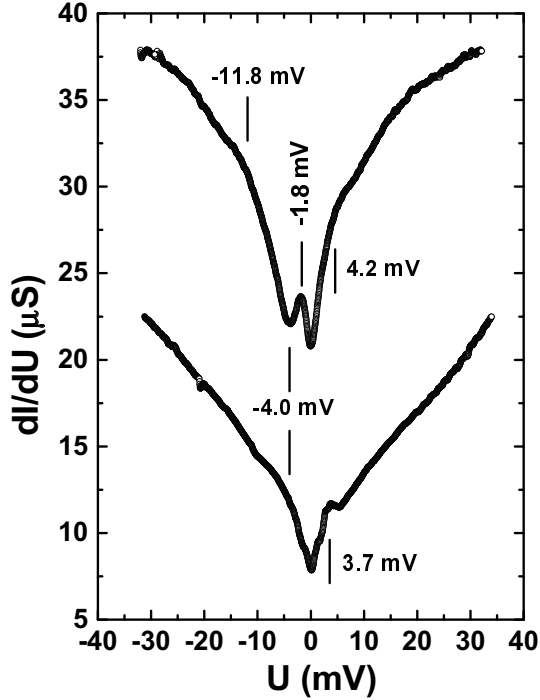


FIG. 5. $dI/dU(U)$ spectra of contacts with medium zero-bias conductance at $T = 0.1$ K. Arrows mark the characteristic energies.

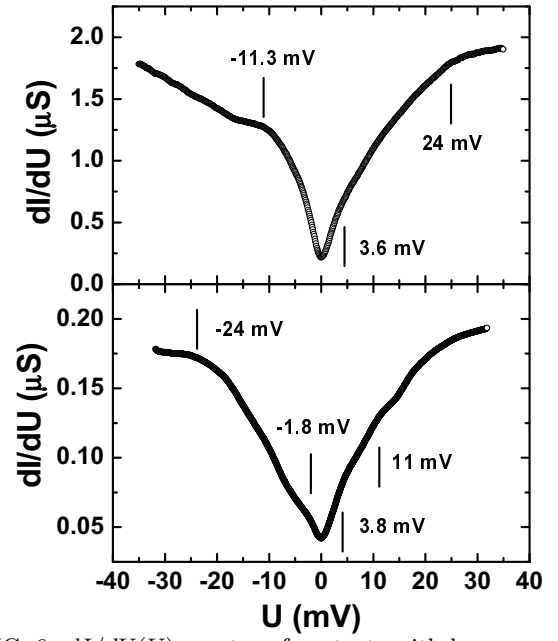


FIG. 6. $dI/dU(U)$ spectra of contacts with low zero-bias conductance at $T = 0.1$ K. Arrows mark the characteristic

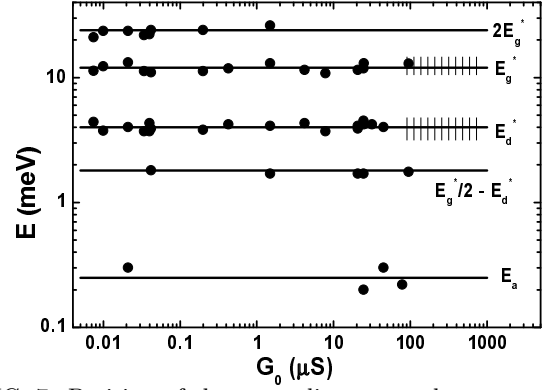


FIG. 7. Position of the anomalies vs. conductance at zero bias voltage. Solid circles represent break-junction data, the shaded area indicates average values derived from the spear-anvil type junctions (for which G_0 is the zero-bias conductance at 4.2 K). Solid lines are guides to the eye, and ten-

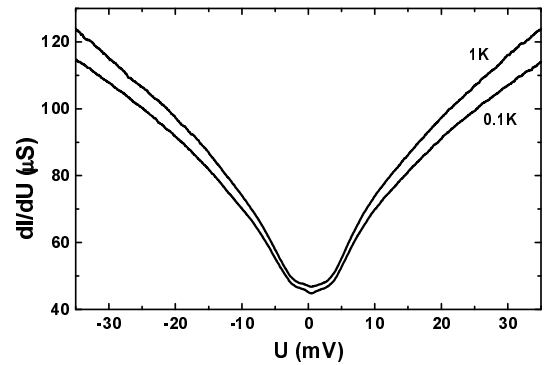


FIG. 8. $dI/dU(U)$ spectra of a contact at $T = 0.1$ K and

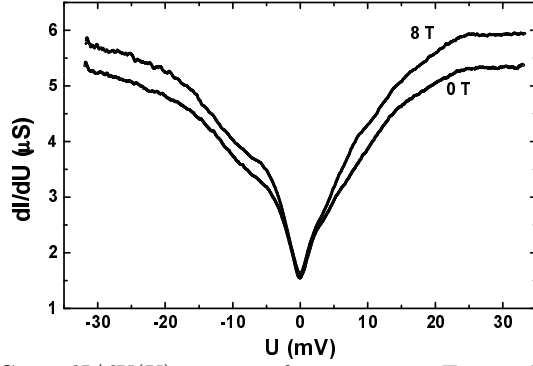


FIG. 9. $dI/dU(U)$ spectra of a contact at $T = 0.1$ K in a magnetic field of 0 T and 8 T.

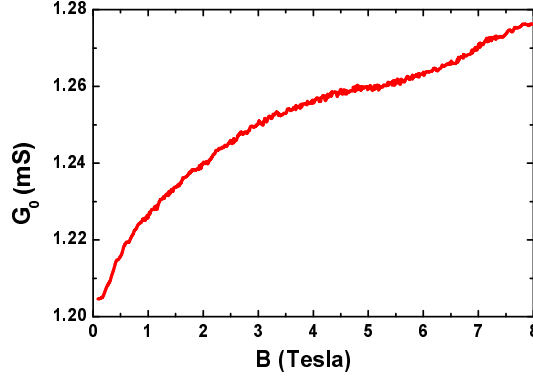


FIG. 10. $G_0(B)$ for a contact at $T = 0.1$ K.

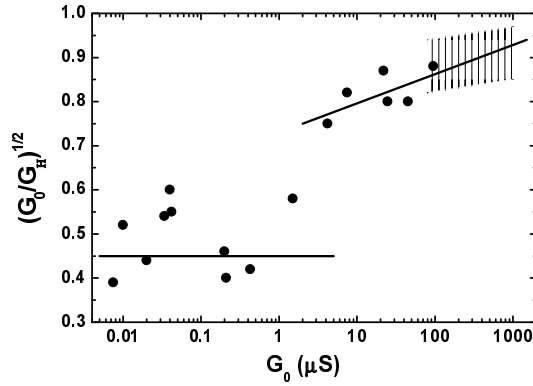


FIG. 11. Square-root of the normalized residual zero-bias conductance $\sqrt{G_0/G_H}$ vs. zero-bias conductance G_0 . Without the gap a zero-bias conductance G_H is estimated. Solid circles represent break-junction data, the shaded area indicates average values derived from the spear-anvil type junctions (for which G_0 is the zero-bias conductance at 4.2 K). The solid lines are guides to the eye.

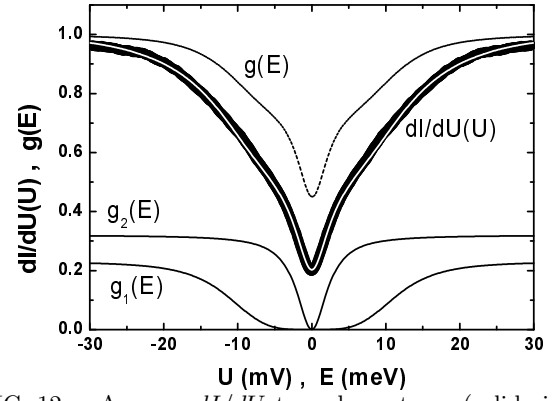


FIG. 12. Average dI/dU tunnel spectrum (solid circles) and a fit (white solid line through the data points) calculated using the density of states $g(E)$ shown by the dotted line. $g(E)$ is the sum of $g_1(E)$ and $g_2(E)$ plus a constant background.

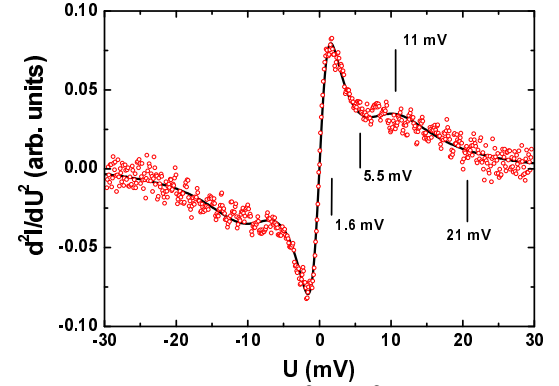


FIG. 13. Second derivative d^2I/dU^2 of the average spectrum of the tunnel junctions (open circles) and of the fit (solid line).